

What is the nature of the C-C complex in silicon? Insights from electronic structure calculations

Dilyara Timerkaeva,^{1,2} Claudio Attaccalite,^{3,4} Gilles Brenet,^{1,2} Damien Caliste,^{1,2} and Pascal Pochet^{1,2}

¹Universit Grenoble Alpes, CS 40700, 38058 Grenoble Cedex, France

²Laboratoire de Simulation Atomistique (L-Sim), MEM, INAC, CEA, 38054 Grenoble Cedex 9, France

³CNRS/Univ. Grenoble Alpes, Institut Néel, F-38042 Grenoble, France

⁴Centre Interdisciplinaire des Nanosciences de Marseille, Aix-Marseille Université, Campus de Luminy, Marseille, 13288 Cedex 09, France

The structure of the C-C complex in silicon has been debated since long time. Different theoretical and experimental studies tried to shed light on the properties of these defects that are at the origin of the light emitting G-center. It is essential to understand structural and electronic properties of these defects because they are relevant for applications in lasing and there is an increasing interest to control their formation and concentration in bulk silicon. In this paper, we study structural, electronic, and optical properties of different possible configurations of the C-C complex in bulk silicon by means of density functional theory (DFT) plus many-body perturbation theory (MBPT). Our findings show that different competing structures could be at the origin of the experimental results.

I. INTRODUCTION

Carbon being an isovalent impurity to silicon initially occupies a substitutional position (C_s). High energy irradiation (electron, ion, proton, or gamma) creates fast diffusing self-interstitials. Some of those interact with carbon atoms and kick them out of the substitutional sites to create carbon interstitials (C_i). C_i is mobile above room temperature and though it interacts with other impurities and forms defect complexes. C_iC_s is one of the secondary irradiation induced defects, which is perhaps the most studied due to its rich physics and interesting structural, electronic, and optical features.

The pair is associated to a G-center which emits light on 0.97 eV (1280 nm).^{1,2} It was discovered in the 60's as a by-product in the silicon crystal caused by the radiation damage from the bombardment with high energy electrons, ions and gamma rays. In recent years, an important effort has been made in order to increase the G-centers concentration¹⁻³. The methods are generally based on the silicon surface alteration, followed by a laser annealing. These technologies have promising applications in development of a silicon laser.

The structure of the complex has been debated for a long time in different experimental and theoretical studies.⁴⁻¹² The early Electron Paramagnetic Resonance (EPR) study⁴ identified a signal, called as Si-G11, that corresponds to a vacancy occupied by two carbon atoms in a positive charge state. The angular dependence in the Si-G11 Zeeman spectrum suggests that two carbon atoms lie in $\langle 110 \rangle$ plane, while the C-C bond is oriented along the $\langle 111 \rangle$ direction. Later experiments, based on optical detection of magnetic resonance (ODMR) study⁵ of the 0.97 eV optical peak, relate the G-center to the C_iC_s complex in its neutral state. O'Donnell *et al.*⁵ proposed another model for C_iC_s complex where the substitutional carbon atoms are separated with interstitial silicon atom. Two modifications of such a complex are

possible: the A-form, when the interstitial silicon is a three bonded, and the B-form, when the Si is bonded to two neighboring C_s atoms. Bistable C_iC_s complex (A- and B-forms on Figures 1a and 1b) and its charged states have been studied experimentally.⁶ Song *et al.*⁶ have performed a wide analysis of a bistable C_iC_s complexes in p- and n-doped silicon by means of EPR, Deep Level Transient Spectroscopy (DLTS) and Photoluminescence spectroscopy (PL) techniques and have provided a complete configurational-coordinate energy diagram. The A-form is found to be lower in energy for all the charged states except neutral where the B-form is slightly lower in energy. Later the Localized Vibrational Modes (LVMs) of the bistable complex have been obtained by means of Infrared (IR) spectroscopy.⁷ The obtained spectra for B-form (540.4, 543.3, 579.8, 640.6, 730.4 and 842.4 cm^{-1}) and A-form (only five of six local modes were identified 594.6, 596.9, 722.4, 872.6, 953.0 cm^{-1}) are in fair agreement with values obtained via *ab initio* calculations^{8,9}.

In 2002, Laiho *et al.*¹⁰ by means of EPR, have detected a new low-symmetry configurations of a complex containing an interstitial silicon and two identical carbon atoms. These signals, named as Si-PT4 and Si-WL5, have not been identified so far, however their presence suggest several forms of C_iC_s complex. These forms appear during the cooling procedure and possess varying magnetic properties.

The exact geometry configurations of carbon-pair can be investigated by first principles studies. A few theoretical attempts have been performed during recent years. By means of DFT calculations, Liu *et al.*¹³ proposed a third configuration of C_iC_s complex (see Figure 1c), the C-form: two carbon atoms are situated in a vacancy and oriented in $\langle 100 \rangle$ direction. Although, the configuration was found to be at least 0.2 eV more stable than A and B for all charge states, there are no experimental observations proving this form presence so far.

Since then, most of the theoretical works investigate the three forms of C_iC_s complexes¹⁴⁻¹⁶ (see Figures 1a,

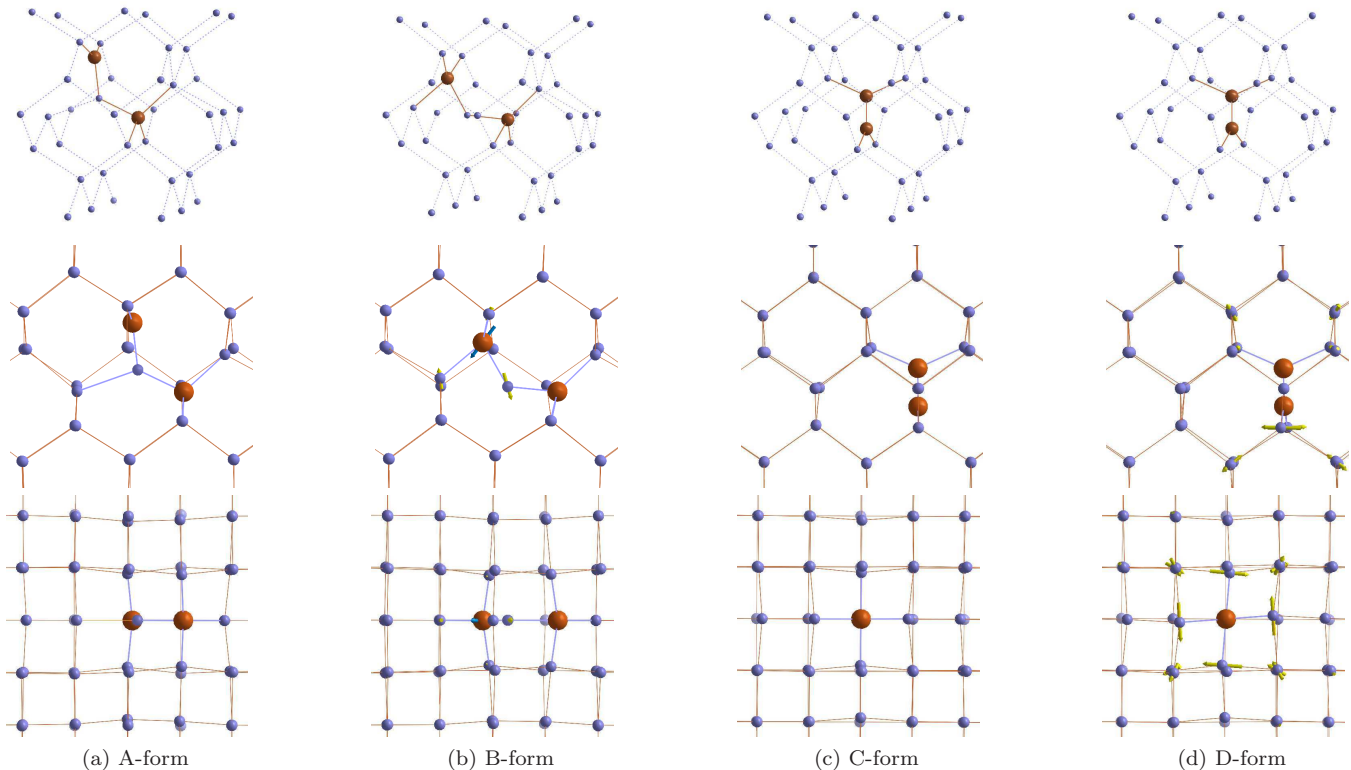


FIG. 1: "Side" view (top line) and "top" view on the four forms of C_2C_s complex. Arrows show the distortion of B-form with respect to A-form and of D-form with respect to C-form.

1b, and 1c). However, their results are not in agreement with each other. Reported by Mattoni *et al.*¹⁴ and Dočaj *et al.*¹⁶, the binding of A-form is as strong as that of C-form, however both of the forms are less stable than B in neutral state. In these two studies, non spin polarized calculations have been performed. In contrary, Zirkelbach *et al.*¹⁵ have calculated the stability of dicarbon pairs by taking the spin into account and have found the C-form the most stable. Finally, we found another stable configuration of C_2C_s complex, which we call as D-form, that is a torsion of C-form along the C-C bond axis (see Figure 1d).

Here, we present our investigation of the structure, vibrational properties, and optical absorption spectra by means of first-principle calculations in order to determine and characterize the different forms of this C_2C_s complex. Moreover, we make an attempt to obtain the ground state (geometries, binding energies) and excited state properties (band gaps and optical absorption/emission spectra) of all the four forms. The latter property could allow us to assign which of four forms corresponds to the light-emitting G-centre.

The paper is organized as follows: in section II we summarize the computation methods employed in the calculation of the atomic structure and the electronic and optical properties; in section III there are the numerical parameters entering in the calculations; in section IV we

present results for electronic structure and optics, and finally in section V we draw the conclusions.

II. METHODS

The defected structures was implanted in silicon super-cells containing 64 (small) and 216 (big) atoms, within periodical boundary conditions. The geometry optimization was performed using BigDFT wavelet based code¹⁷ with Hartwigsen-Goedecker-Hutter pseudo-potentials¹⁸ and the GGA-PBE functional.¹⁹ To reach the local minima of every structure we used the Fast Inertial Relaxation Engine (FIRE).²⁰ Variations in geometry structures of the defects of interest in the small and big super-cells are negligible. However the energies of the various structures slightly differ. In addition, an accurate prediction of excited state properties requires accounting the long-range interactions. Thus considering big super-cells is crucial and all further results were obtained in the large super-cells. To calculate the phonon modes, we employed the finite difference method within the frozen phonon approximation. To accelerate computations, a defect and its first-shell neighbors were considered exactly, while the remote atoms were contributing as unperturbed bulk atoms.

Then, we took optimized structures and generate oc-

cupied and empty states²¹ with the plane-wave based code QuantumEspresso²², the norm-conserving Troullier-Martins pseudo-potentials²³ and PBE functional.¹⁹

Then we correct the Kohn-Sham levels by means of many-body perturbation theory in order to obtain the quasi-particle(QP) band structure and the optical response of the system. The quasi-particle band structures are obtained within the GW approach.²⁴ Specifically, we use non-self consistent GW (denoted as G_0W_0) in which the screened Coulomb potential, W , and the Green's function, G , are built from the KS eigenstates $\{\varepsilon_{n\mathbf{k}}; |n\mathbf{k}\rangle\}$ (with \mathbf{k} the crystal wave vector and n the band index). The quasi-particle energies are then obtained from:

$$\varepsilon_{n\mathbf{k}}^{\text{QP}} = \varepsilon_{n\mathbf{k}} + Z_{n\mathbf{k}} \Delta \Sigma_{n\mathbf{k}}(\varepsilon_{n\mathbf{k}}). \quad (1)$$

In Eq. 1

$$Z_{n\mathbf{k}} = [1 - \partial \Delta \Sigma_{n\mathbf{k}}(\omega) / \partial \omega |_{\omega = \varepsilon_{n\mathbf{k}}}]^{-1},$$

is the re-normalization factor and

$$\Delta \Sigma_{n\mathbf{k}} \equiv \langle n\mathbf{k} | \Delta \Sigma | n\mathbf{k} \rangle,$$

where

$$\Delta \Sigma = \Sigma - V^{\text{xc}},$$

is the difference between $\Sigma = GW$, the GW self-energy, and V^{xc} , the exchange-correlation potential used in the KS calculation.²⁵

The optical-spectra are calculated by solving the Bethe-Salpeter equation (BSE):²⁶

$$\sum_{v'c'k'} (\varepsilon_{c\mathbf{k}}^{\text{QP}} - \varepsilon_{v\mathbf{k}}^{\text{QP}}) A_{vc\mathbf{k}}^s + \sum_{v'c'k'} \langle v\mathbf{k} | K_{eh} | v'\mathbf{k}' \rangle A_{v'c'\mathbf{k}'}^s = \Omega^s A_{vc\mathbf{k}}^s. \quad (2)$$

Here, the electronic excitations are expressed in a basis of electron-hole pairs $|v\mathbf{k}c\rangle$ corresponding to transitions at a given \mathbf{k} from a state in the valence band (v) with energy $\varepsilon_{v\mathbf{k}}^{\text{QP}}$ (hole) to a conduction-band (c) state with energy $\varepsilon_{c\mathbf{k}}^{\text{QP}}$ (electron). $A_{vc\mathbf{k}}^s$ are the expansion coefficients of the excitons in the electron-hole basis and the Ω^s are the excitation energies of the system. In case of spin-polarized defects we performed spin-polarized calculations both at the GW and BSE level.

III. CALCULATION DETAILS

In this section we report the convergence parameters that enter in each of calculations discussed in the previous section.

Structure optimization has been performed using a 0.42 Bohr grid spacing on the wavelet mesh and then in plane-wave we used a cutoff of 80 Ry to generate the KS wave-functions. In the G_0W_0 calculation, we used 1500 bands

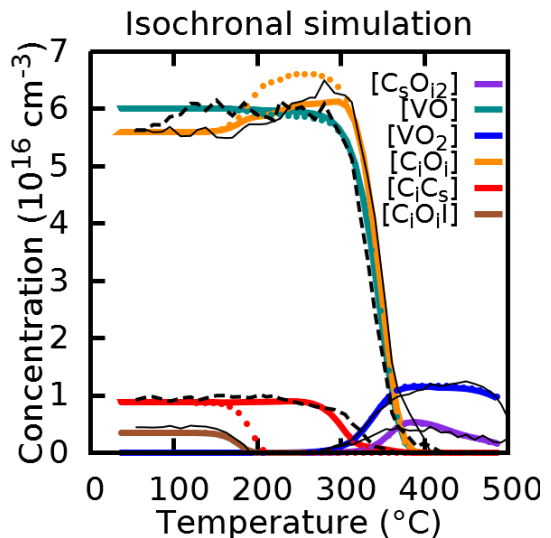


FIG. 2: [Color online] Isochronal annealing of carbon/oxygen related defects in silicon. Colored lines are simulated curves, with the C-form of C_iC_s for plain lines and the B-form for the dotted lines. The black lines represent experimental values.

for the expansion of the Green's functions and for the calculations of the screened interaction W , 30.000 G -vectors to expand the Kohn-Sham orbitals, 2 Ha cutoff for the G -vectors entering in the dielectric constant. The dielectric constant entering in the definition of W has been calculated using a double-grid technique to integrate in the Brillouin Zone with a single k -point (gamma point) for the matrix elements and a $2 \times 2 \times 2$ shifted grid for the single-particle energies, see Ref. 27 for details. The same double-grid technique has been used in the calculation of the optical response. For the BSE we used the static part of the screening calculated in the GW , 100 valence bands and 100 conduction bands for the calculation of the optical absorption, and 15.000 G -vectors to describe the Kohn-Sham wave-functions. Then the BSE equation has been inverted and interpolated on the double grid too.²⁷ All the GW and BSE calculations have been performed with the Yambo code.²⁸

IV. RESULTS AND DISCUSSION

In this section we will address the structural, vibrational, electronic and optical properties of the different C_iC_s complexes.

a. Structure and binding energies of the various forms of the C_iC_s complex In Figures 1a - 1d, the four obtained optimized configurations of C_iC_s complex are shown. In the A-form, carbon atoms occupy neighboring lattice sites, while the Si atom is an interstitial bonded to both carbon atoms and one silicon. The B-form is similar to A but the interstitial Si only bridges the two carbon

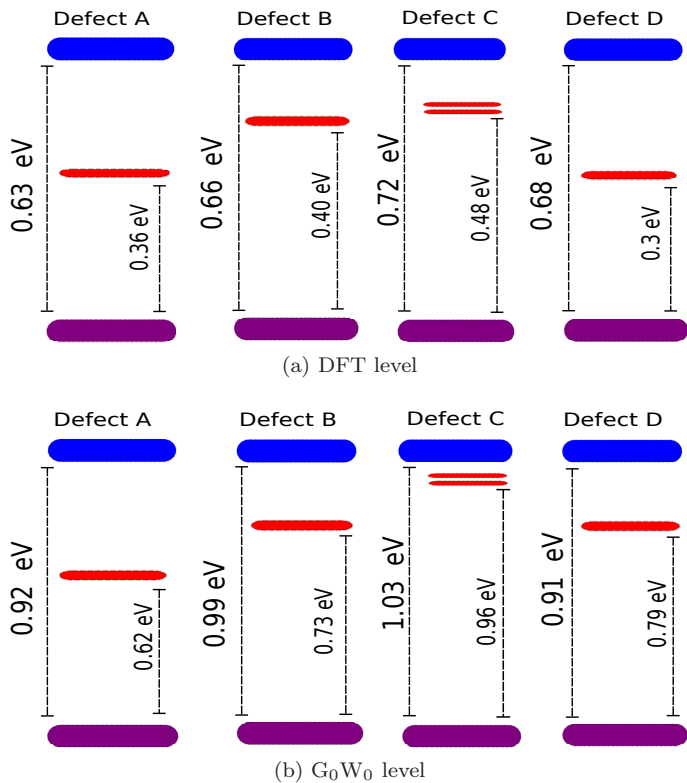


FIG. 3: [Color online] Schematic band structure of the defects levels in the different complexes.

atoms and are not bonded to another Si. The third configuration consists of two carbons in a vacancy aligned in a (100) crystallographic direction. D-form slightly differs from the previous configuration: all Si atoms bonded to two C atoms are slightly twisted around a C-C axis. D-form was obtained through non-spin-polarized geometry optimization. The initial configuration for this optimization was chosen to be slightly different from the C-form. Thus, we can conclude, that D-form is another local minima, which is similar to the C-form but almost 0.4 eV higher in energy.

The twisted shape of the D-form can result from the rotation of π -orbitals of two C atoms in order to form a π bond (see Figures 1c and 1d). In the C-form, the two corresponding π -orbitals are perpendicular to each other; each of them is occupied by one electron, making this complex paramagnetic.

All four forms of C_iC_s complex can be created from very same ingredients, *i.e.* from mobile interstitial carbon and immobile carbon in substitution. Depending on the topology of the reaction, either A and B or C and D forms can be reached. In a neutral state, A will directly transform to B, as B is more stable. The A to B transformation barrier has been estimated to be as low as 0.1 eV¹⁵. Transformation from either A (or B) to C and backward is less probable as the transformation barrier have been estimated to be as high as 2-3 eV¹⁶. Nevertheless, the kinetics of C_iC_s complex formation and re-

orientation, *i.e.* various migration barriers, is out of the range of the present study. Interested readers can find information in the work of Zirkelbach *et al.*¹⁵.

The binding energies of the complex were calculated as $E_b(C_iC_s) = -E_{tot}(215SiC_iC_s) - E_{tot}(216Si) + E_{tot}(215SiC_s) + E_{tot}(216SiC_i)$ and the obtained values are listed in Table I. The C-form is found to be the most stable among all. These results are in contradiction with some recent theoretical studies^{14,16} however it is in agreement with findings of Zirkelbach *et al.*¹⁵ and Liu *et al.*¹³. We demonstrate the crucial role of the spin in complex respective stabilities, as it increases the binding energy by about 0.17 eV compare to non-spin polarized calculations (0.2 eV in Ref.¹⁵). The D configuration has a binding energy of 0.88 eV, which is close to that of A-form.

E_b , eV	This work	Ref.15	Ref.16	Ref.14	Ref.8	Ref.9	Ref.13
A-form	0.86	0.93	0.92	w	x-0.35	y-0.11	z-0.2
B-form	0.93	0.95	1.28	w-0.4	x	y	z-0.2
C-form	1.11		0.90	w-0.2			
C-form(SP)	1.28	1.28					z
D-form	0.88						

TABLE I: Binding energies in eV for four configurations of C_iC_s . Some authors have only reported relative values. That is why, energies of the most stable configurations from References^{14, 8, 9, and 13} are indicated with letters *w*, *x*, *y*, and *z*, respectively. SP states for spin polarized calculations.

Generally speaking, all these forms can be present in a heavily carbon doped silicon, and their relative concentrations should depend on their binding energies. It should be also taken into account, that formation kinetics can impact significantly the balance between the four complex concentrations. That is why, even if the A- and B-forms are indeed less stable than the C-form, they could be present in the sample and could be detected by various experimental techniques, such as IR and EPR spectroscopy.

In experiments, a 546 cm⁻¹ band is used to measure the C_iC_s complex concentration. The Figure 2 shows the concentrations of various carbon related defects in silicon during an isochronal annealing (20 min). Those concentrations are extracted from Kinetic Mass Action Law (KMAL) simulations²⁹ for the colored lines, and from the experiment^{30,31} for the black lines. Two different simulations were made: the curve in plain lines takes into account the binding energy of the C-form of C_iC_s ($E_b = 1.28$ eV), whereas the one in dotted lines takes into account the binding energy of the B-form ($E_b = 0.93$ eV).

The two simulations exhibit the main features of the experiment: species, their concentrations, and the reaction temperatures. The only difference between the two simulations is the binding energy of C_iC_s pair. While

considering the C-form, the simulation reproduces two following experimental parameters: first, the C_iC_s dissociation temperature of 280-300 °C; second, the experimentally observed evolution of C_iO_i pair. These evidences favor the C-form existence. While considering the B-form, the decay of C_iC_s pairs at lower temperatures (190 °C) liberates the mobile C_i species, causing the rise in C_iO_i concentration just before its dissociation. This rise is not seen experimentally, adding a further proof that the C-form is the one detected in this experiment.

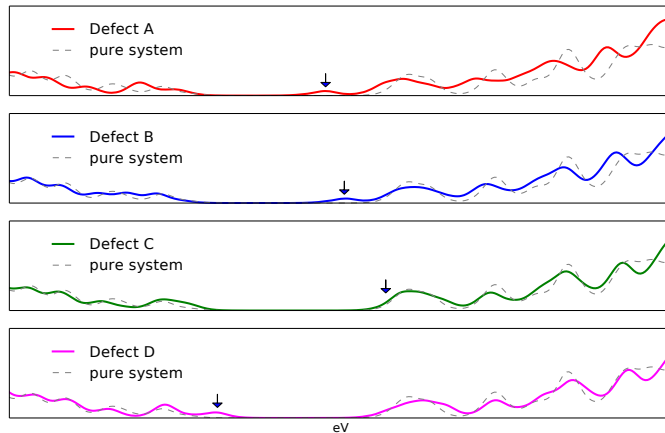


FIG. 4: [Color online] Density of states at the G_0W_0 level, in presence of the different defect complexes, compared with the one of the bulk silicon with the same supercell. The arrows indicate the position of the defects deep-levels in the band gap.

The just described observation is a strong evidence for the presence of the C-form in irradiated silicon, but more detailed analysis of other properties should be performed in order to finally assign the observed properties of dicarbon pair to any of its form. Hereafter, we will consider four forms of C_iC_s pair, namely A-, B-, magnetic C-, and D-form, as far as they are the most interesting configurations. Particularly, we will define their vibrational and excited states properties.

b. Vibrational properties One of the easiest ways to decipher the exact configuration of defects presented in a sample is a combined theoretical-experimental investigation of LVMs. An accordance between the obtained values would unambiguously point a correct structure, while lines' intensity would give an estimation of concentration. Therefore, we present here our theoretical investigation of LVMs of the four forms of C_iC_s and will compare them with already published results (see Table II). Our values for the A- and B- forms are in excellent agreement with experiment and previous calculations. For the C-form our results differs in larger extend. This can be related to the differing geometries of the C-form between our and Docaj's study.¹⁶ Spin polarization was not taken into account in the study of Docaj, thus they could deal with the D-form or another local minimum. The obtained results can be a reference point for future IR experiments,

indicating the energy range for a possible LVM bands of the C-form. For example, in the study of Lavrov *et al.*⁷, there was an assumption, that only B form is existing in neutral form, that is why the reported IR spectra were ranged up to 1000 cm^{-1} and above 7000 cm^{-1} . While according to our calculations the highest frequency of C-form correspond to 1135 cm^{-1} and is obviously out of the scope of the just mentioned work.

c. Electronic and optical properties While the situation is rather clear with LVM fingerprints, which is hard to misinterpret, more attention should be paid to the formation kinetics and optical properties of the forms of carbon-carbon pair. We start our discussion of the electric properties of the four complexes at the Kohn-Sham level. In Figure 3a we report a schematic representation of the electronic band structure of the four defects. We found that although we use a large supercell, more than 200 atoms, the presence of the defects slightly affect the bulk gap, by about 0.13 eV in the worst case of the complex A, due to resonant defect states. We found that the four complexes present deep levels in the band gap. In the A, B and D cases there is a single level inside the gap situated respectively at 0.36 eV, 0.40 eV and 0.30 eV from the top valence band. The C case is different because the defect is spin-polarized and therefore the level in the gap is split into two levels one for each spin polarization. Finally, we have to mention that in the D complex there is a strong resonance close to the top valence bands, that generates a strong absorption peak at high frequencies as we will see in the following. Then we turn on quasi-particle correction and obtain the band structure schematically reported in Figure 3b.

The GW correction opens the gap from 0.76 eV to 1.1 eV and also raises the deep level positions respect to the top valence bands. In the A,B and D cases these levels remain in the band gap while in the C case the two levels almost merge with the bottom of the conduction bands (see Figures 3a and 4). This fact has important implications on the optical properties as we will see in the following. Beyond the shift of the electronic levels. The corresponding density of states (DOS), calculated using a $2 \times 2 \times 2$ shifted grid plus the gamma point, is reported in Figure 4. We compare the DOS of the four defected structures with the one of the pure system aligning the top valence band position. The DOS of the four complexes are similar to the one of the pure system but the peaks are smoother because of the presence of defects that breaks symmetries in the supercell. In the band gap the deep levels are clearly visible, except for the C case, where DOS generated by defect levels merges with the one of the conduction DOS. Now that we have analyzed the electronic structure of the four defects we move to their optical properties.

The optical response was evaluated by means of the GW plus Bethe-Salpeter equation (BSE), *i.e.* including both local-field effects and electron-hole interaction, see Figure 5.

Since we would like to compare the optical properties

this study				Docaj ¹⁶			Leary ⁸	Capaz ⁹	Lavrov ⁷		Lavrov ³²	
theory				theory			theory	theory	experiment	experiment		
A	B	C-SP	D	A	B	C-NSP	B	A	B	A	B	N/A
933	819	1135	1182	917	805	1181	838	890	841	953	842	749
861	702	801	744	912	704	810	715	874	716	873	730	527
699	608	733	732	710	663	806	649	722	643	722	641	
572	548	549	525	598	567	580	582	567	567	597	580	
566	525			591	563		552	557	514	594	543	
	521				549		543		503		540	

TABLE II: Frequencies in cm^{-1} of the three A,B and C forms of C_iC_s pair.

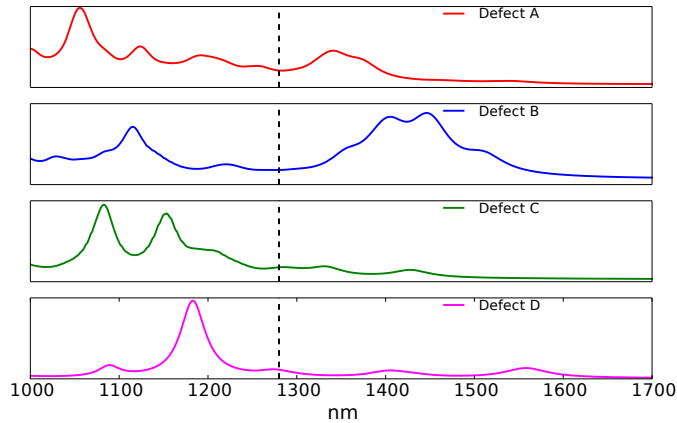


FIG. 5: [Color online] Optical absorption in presence of the different defect complexes with the G_0W_0 approximation plus the Bethe-Salpeter equation. The vertical lines are the experimental light emission^{1,2}

with light emission experiments we will discuss here only the lowest absorption peaks of the four complexes, the ones affected by the presence of the defects. The optical spectra at the Independent Particle Approximation (IPA) level, can be easily deduced from the band structure. Correlation effects modify the spectra in two ways: first the GW corrections shift the level positions and second the BSE mixes the single particle transitions and redistribute the spectral weight. In the case of the B complex these effects just modify the shape of the spectra leaving the lowest absorption peak around 1450 nm. In the A case there is strong redistribution of the spectral weight, the peak at 1300 nm disappears and the peak at 1350 nm acquires more strength. But the C and D cases are the one most affected by the GW corrections (see schematic band structure 3b). In fact the deep levels of the C complex are pushed up by GW correction and so the absorption peaks move to lower wave-lengths. In the D case the peak at high energy is shifted toward lower frequencies. Fig. 5 illustrates the situation, now lowest absorption peaks of the C complex are at 1080 nm and 1150 nm while the one of the D complex is around 1180 nm. The final outcome of these results is that now the absorption peaks of the A and B complexes are too

high in wavelengths to explain the G-center emission, while the C and D remain close to the emission measured in the experiments.

V. CONCLUSIONS

In this paper we have performed a detailed investigation on the properties of the forms of the C_iC_s complex from first principles calculations. We intend to better understand what are the properties of the possible forms of C_iC_s complex and why the C-form, which is the most stable according to our calculations, has been never experimentally observed so far. In addition, we tried to characterize theoretically the optical properties of the four forms of carbon-carbon pair, and assign one of them to the light emitting G-centre.

First, we found that among all four C_iC_s forms, the C-form is the most stable, as it's binding energy is 0.4 eV higher than that of the B-form. Moreover, KMAL isochronal annealing simulations show that the dissociation temperature of 546 cm^{-1} band, that is used to determine the stability of C_iC_s complex, corresponds to the binding energy of the C-form. Meanwhile, that of the B-form lead to a dissociation at about 100 °C lower in temperature, which leads to a strong disagreement with experiment and therefore becomes another evidence for the C-form existence. Second, we attribute a set of localized vibrational modes to each of four configurations. The set corresponding to the C-form contains four bands, three of which are at the range of those of A- and B-forms, and can be overlapped with those. The highest band of 1135 cm^{-1} is above the registration range of most LVM experiments, thus it could be missed during measurements. Then we studied electronic and optical properties of the C_iC_s complexes. We found that the inclusion of correlation effects is crucial to describe the optical properties of C-C defect complexes. In fact, the different approximation in standard semi-local functionals fail to describe the correct level position of localized and resonant defect states respect to the bulk levels. Therefore, we provide here an accurate quasi-particle band structure of the four complexes and their optical absorption with the GW+BSE approximation. Regarding now the form re-

sponsible for the light emitting G-centre, C and D configurations are better candidates for the light emission band at 1280 nm. To conclude, all these facts become strong evidence of the existence of the C- and D-forms of C_iC_s in heavily carbon doped silicon.

Up to our knowledge, no evidences of C-form have been obtained by the Electronic Paramagnetic Resonance technique, which is another effective characterization method. However, as the C-form is a magnetic complex according to our simulations, its signal should lie in a range of the spectra, situating far from the signal of neutral species. Hence, additional characterization experiments are necessary, in order to investigate the C

and D configurations. New experiments should account for the complexes' vibrational properties, obtained in the current study, as well as their magnetization.

VI. ACKNOWLEDGMENTS

Computing time has been provided by the national GENCI-IDRIS and GENCI-TGCC supercomputing centers under contracts n° t2012096655 and n° t2014096107.

-
- ¹ D. Berhanuddin, M. Lourenco, C. Jeynes, M. Milosavljević, R. Gwilliam, and K. Homewood, *Journal of Applied Physics* **112**, 103110 (2012).
 - ² D. D. Berhanuddin, M. A. Lourenço, R. M. Gwilliam, and K. P. Homewood, *Advanced Functional Materials* **22**, 2709 (2012).
 - ³ K. Murata, Y. Yasutake, K.-i. Nittoh, S. Fukatsu, and K. Miki, *AIP Advances* **1**, 032125 (2011).
 - ⁴ K. L. Brower, *Phys. Rev. B* **9**, 2607 (1974).
 - ⁵ K. O'Donnell, K. Lee, and G. Watkins, *Physica B+ C* **116**, 258 (1983).
 - ⁶ L. W. Song, X. D. Zhan, B. W. Benson, and G. D. Watkins, *Phys. Rev. B* **42**, 5765 (1990).
 - ⁷ E. V. Lavrov, L. Hoffmann, and B. B. Nielsen, *Phys. Rev. B* **60**, 8081 (1999).
 - ⁸ P. Leary, R. Jones, S. Öberg, and V. J. B. Torres, *Phys. Rev. B* **55**, 2188 (1997).
 - ⁹ R. B. Capaz, A. Dal Pino, and J. D. Joannopoulos, *Phys. Rev. B* **58**, 9845 (1998).
 - ¹⁰ R. Laiho, M. Vlasenko, and L. Vlasenko, *Solid State Communications* **124**, 403 (2002).
 - ¹¹ H. Wang, A. Chroneos, C. A. Londos, E. N. Sgourou, and U. Schwingenschlögl, *Scientific Reports* **4**, 4909 (2014).
 - ¹² H. Wang, A. Chroneos, C. A. Londos, E. N. Sgourou, and U. Schwingenschlögl, *J. Appl. Phys.* **115**, 183509 (2014).
 - ¹³ C.-L. Liu, W. Windl, L. Borucki, S. Lu, and X.-Y. Liu, *Applied Physics Letters* **80**, 52 (2002).
 - ¹⁴ A. Mattoni, F. Bernardini, and L. Colombo, *Phys. Rev. B* **66**, 195214 (2002).
 - ¹⁵ F. Zirkelbach, B. Stritzker, K. Nordlund, J. K. N. Lindner, W. G. Schmidt, and E. Rauls, *Phys. Rev. B* **84**, 064126 (2011).
 - ¹⁶ A. Docaj and S. Estreicher, *Physica B: Condensed Matter* **407**, 2981 (2012).
 - ¹⁷ L. Genovese, A. Neelov, S. Goedecker, T. Deutsch, S. A. Ghasemi, A. Willand, D. Caliste, O. Zilberberg, M. Rayson, A. Bergman, *et al.*, *The Journal of chemical physics* **129**, 014109 (2008).
 - ¹⁸ M. Krack, *Theoretical Chemistry Accounts* **114**, 145 (2005).
 - ¹⁹ J. P. Perdew, K. Burke, and M. Ernzerhof, *Phys. Rev. Lett.* **77**, 3865 (1996).
 - ²⁰ E. Bitzek, P. Koskinen, F. Gähler, M. Moseler, and P. Gumbach, *Phys. Rev. Lett.* **97**, 170201 (2006).
 - ²¹ We checked that the optimized structures did not significantly change if we reoptimize them using plane-waves and Troullier-Martins pseudopotentials.
 - ²² P. Giannozzi *et al.*, *J. Phys. Condens. Matter* **21**, 395502 (2009), <http://www.quantum-espresso.org>.
 - ²³ N. Troullier and J. L. Martins, *Phys. Rev. B* **43**, 1993 (1991).
 - ²⁴ F. Aryasetiawan and O. Gunnarsson, *Rep. Prog. Phys.* **61**, 237 (1998).
 - ²⁵ W. G. Aulbur, L. Jonsson, and J. W. Wilkins, *Solid State Physics* (edited by H. Ehrenreich and F. Spaepen), Academic press **54**, 1 (1999).
 - ²⁶ G. Strinati, *Riv. Nuovo Cimento* **11**, 1 (1988).
 - ²⁷ D. Kammerlander, S. Botti, M. A. L. Marques, A. Marini, and C. Attaccalite, *Physical Review B* **86**, 125203 (2012).
 - ²⁸ A. Marini, C. Hogan, M. Grüning, and D. Varsano, *Computer Physics Communications* **180**, 1392 (2009).
 - ²⁹ G. Brenet, D. Timerkaeva, E. N. Sgourou, C. A. Londos, D. Caliste, and P. Pochet, *J. Appl. Phys.* **118**, 125706 (2015).
 - ³⁰ E. Sgourou, D. Timerkaeva, C. Londos, D. Aliprantis, A. Chroneos, D. Caliste, and P. Pochet, *Journal of Applied Physics* **113**, 113506 (2013).
 - ³¹ C. Londos, E. Sgourou, D. Timerkaeva, A. Chroneos, P. Pochet, and V. Emtsev, *Journal of Applied Physics* **114**, 113504 (2013).
 - ³² E. V. Lavrov, B. B. Nielsen, J. R. Byberg, B. Hourahine, R. Jones, S. Öberg, and P. R. Briddon, *Phys. Rev. B* **62**, 158 (2000).